Journal of the European Ceramic Society 20 (2000) 1339–1344

Crack-location-dependent *R*-curve behavior in Si_3N_4

Jianghong Gong *, Zhenduo Guan

Department of Materials Science and Engineering, Tsinghua University, Beijing 100084, PR China

Received 23 March 1999; received in revised form 2 November 1999; accepted 12 November 1999

Abstract

The rising crack resistance (*R*-curve) behavior in a hot-pressed Si_3N_4 with an elongated grain structure was studied by observing the stable growth of annealed indentation-induced cracks during the bending test. The experimental data corresponding to each individual crack were analyzed according to an exponential function proposed by Ramachandran and Shetty. [Ramachandran, N. and Shetty D. K., Rising crack growth-resistance (*R*-curve) behaviour of toughened alumina and silicon nitride. *J. Am. Ceram. Soc.*, 1991, **74,** 2634–2641]. It was found that the measured *R*-curve is strongly dependent on the crack location. Due mainly to the existence of a microstructural driving force for crack growth, all cracks may start to propagate at nearly the same level of the applied stress intensity. During the subsequent stable growth, however, the variations of crack resistance with crack extension may be different for different cracks located in different sites of the surface of material. The effect of the random orientation of the elongated grains within the material on the interaction between the bridging grain and the propagating crack was suggested to be the main cause of the crack-location-dependence of the measured *R*-curve behavior.

Keywords: Fracture; Si_3N_4; Toughness and toughening; R-curve

1. Introduction

Recent studies have shown that a variety of ceramic materials possess a strong *R*-curve property, i.e. they exhibit increasing resistance to fracture with crack extension.[1-4] *R*-curve behavior may be induced by mechanisms such as transformation or crack-bridging which "shield" the crack tip from external loads[5,6] and then provide flaw tolerance characteristics to ceramics and narrow their strength distribution.[7,8]

It is most desirable to study the *R*-curve behavior of ceramics by observing the stable growth of the preexisting defects or flaws which actually cause failure in service. However, such a study is not tenable for it is usually difficult to locate and monitor the flaws that eventually lead to fracture.[1,2] To overcome this difficulty, an indentation-crack growth method has been developed and frequently employed to measure the *R*-curve behavior for ceramics.[9–12] Similar to the "Modified Indentation Method" proposed by Cook and Lawn[13] for determining the toughness, the indentation-crack growth method uses a series of Vickers indentations placed within the uniformly stressed region of the tensile surface of a four-point bending specimen. Then, the specimen is incrementally loaded and the stable extension of the indentation-induced cracks in response to the applied stress is observed and recorded to establish the *R*-curve. The main advantages of this method are the relative simplicity, small specimen size required and the fact that the indentation-induced cracks are similar to the "natural" flaws preexisting in the materials in both shape and dimension.

In the previous studies on the determination of *R*-curves with the indentation-crack growth method, all the experimental data measured from different indentation cracks in different specimens for a given material were usually presented together in a single crack resistance versus crack size (K_R–c) plot and statistically fitted to a single curve.[9–12] Little attention has been paid to the comparison between the *R*-curves measured respectively with each individual crack. Note that the *R*-curve behavior has been proven to be a microstructure-dependent phenomenon[5,6] and, when examined at the microstructural level, any polycrystalline ceramic should be considered to be inhomogeneous. One can expect that different cracks, which are placed in different

* Corresponding author.
E-mail address: gong@tonghua.com.cn (J. Gong).

0955-2219/00/$ - see front matter
PII: S0955-2219(00)00019-4

specimens of a given material and/or located in different sites in a given specimen, may encounter different variations in crack resistance during extension. The aim of the present paper is thus to explore the effect of crack location on the *R*-curve behavior measured with the indentation-crack growth method. A hot-pressed Si_3N_4 with an elongated grain structure was selected for this study, for it has been established[14,15] that this new generation of material exhibits a strong *R*-curve property due mainly to crack bridging by the elongated β-Si_3N_4 grains.

2. Experimental

Powder mixture of 80 wt% Si_3N_4 with 7.8 wt% Y_2O_3, 11.3 wt% La_2O_3 and 0.9 wt% Al_2O_3 was ball-milled in ethanol with Si_3N_4 grinding balls for 24 h. The milled slurry was dried, sieved through a 50-mesh screen, uniaxially pressed at about 50 MPa to form discs of about 105 mm diameter and about 6 mm thick. The green compacts were then hot-pressed at 1825°C and 25 MPa pressure, using graphite dies and under a nitrogen atmosphere.

Fig. 1 shows the SEM micrograph of a typical microstructure of a polished and etched (HF acid for about 1 h) surface of the final product. As shown, the hot-pressed material has a microstructure consisting of elongated grains.

Four-point bending specimens with nominal dimensions of 35 mm long, 5 mm wide and 2.5 mm thick were cut from the as-hot-pressed material with the tensile surface perpendicular to the hot-pressing direction. All surfaces of the specimens were ground and the edges of the tensile surface were chamfered slightly to eliminate the edge effect. The tensile surface of each specimen was polished carefully to a mirror finish. Three well-developed indentation cracks were produced, each at least 2 mm apart, in the uniformly stressed region of the well-polished tensile surfaces of each specimen by Vickers indentation at room temperature. Great care was taken to ensure that one set of the radial cracks in each indentation was perpendicular to the tensile stress direction in bending. Different indentation loads, 196, 245 and 294 N, were used for indenting different specimens. After being indented, all specimens were annealed at 1000°C in nitrogen atmosphere for 10 min. No crack healing was observed during annealing. The lengths of the surface cracks measured after annealing were somewhat larger than those measured before annealing. This increase in crack dimensions may be attributed to the relief of the residual surface stresses, which were usually compressive, introduced during the machining and polishing of the specimens.

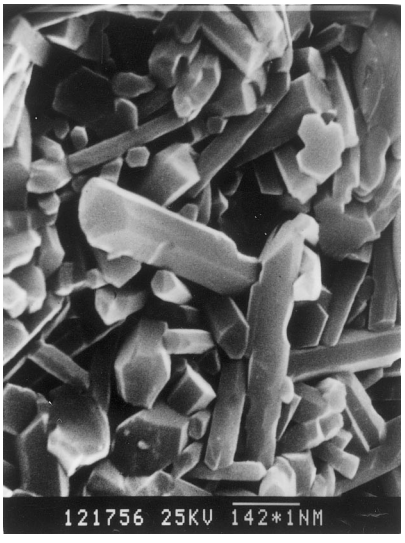

Fig. 1. Microstructure of the test material.

The crack growth measurements were performed at room temperature in a four-point bending fixture with an inner span of 10 mm and an outer span of 30 mm. Specimens were incrementally stressed until one of the three cracks in the specimen reached the critical state. The specimens were stressed to the predetermined peak stress with a crosshead speed of 0.05 mm/min and unloaded quickly after the predetermined peak stress was held for 10 s. After each stress increment, the specimen was removed from the fixture and the crack length was measured using optical microscopy.

Some of the fractured specimens with the remaining indentation-induced cracks were etched in HF acid for about 1 h to expose the microstructure-crack interaction using scanning electron microscopy.

3. Calculation of crack resistance

In general, the total stress intensity, K_I, for an indentation-induced crack in bending can be expressed as the sum of contributions from the applied bending stress, the residual contact stress due to indentation and the residual surface stress due to machining. In the present study, we assumed that both the residual contact stress and the residual surface stress were eliminated completely by annealing. Thus, the actual K_I can be determined as only the applied stress intensity, K_a, through the equation[16]

$$K_I = K_a = Y\sigma\sqrt{c} \quad (1)$$

where σ is the applied bending stress, c is the crack half-length, and Y is the shape factor of crack geometry which can be calculated with the empirical equations proposed by Newman and Raju.[16]

In testing a material with *R*-curve behavior, an incremental crack extension may occur when the stress intensity, K_I, at the tip of the indentation crack is larger

than the crack resistance, K_R, and a quasi-static equilibrium will be attained at $K_I = K_R$. Thus, the crack resistance, K_R, can be calculated directly with Eq. (1) corresponding to each loading–unloading cycle described in Section 2.

Calculating the shape factor of crack geometry, Y, in Eq. (1) needs a knowledge of the ellipticity, i.e. the ratio of the crack depth, a, to the crack half-length, c, of the indentation-induced crack. It has been generally suggested[17,18] that the shape of an indentation-induced crack subjected to bending changes from semicircular to semielliptical as the crack depth increases. In the present study, no experiment was conducted to determine the variation of the crack ellipticity during stable extension. As a reasonable approximation, we estimated the crack ellipticity, a/c, with the assumption proposed by Li et al.,[3]

$$\frac{a}{c} = 1.2 - 0.2\left(\frac{c}{c_0}\right) \tag{2}$$

where c_0 is the initial value of the crack half-length.

4. Results and discussion

Fig. 2 shows the measured crack resistance as a function of the crack length for hot-pressed Si_3N_4. In this figure, the data corresponding to each of the nine symbols represent a set of results measured with each individual crack. As shown, the crack resistance corresponding to each individual crack increases gradually and continuously with crack extension, but significant deviations exist between the shapes and the locations of the R-curves measured with different cracks. Such an experimental phenomenon is somewhat similar to those observed by using the long-crack techniques, such as the single-edge notched beam (SENB) method.[19] Large

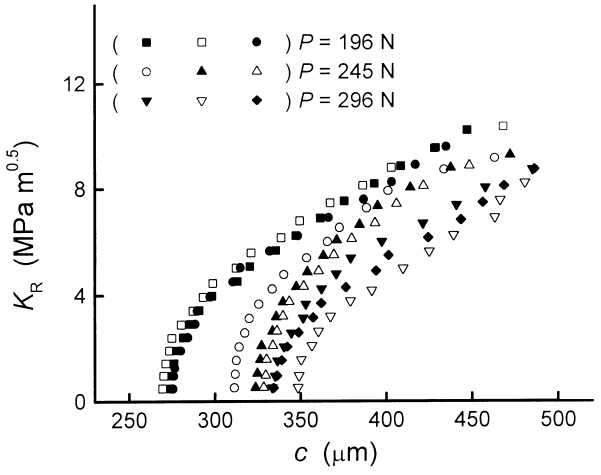

Fig. 2. Crack resistance measurements as functions of crack lengths for indentation-induced cracks with different initial lengths.

scatters in the measured crack resistance have also been reported by other authors when using a similar indentation-crack growth method, in which as-indented specimens were used for the crack growth measurements, to observe the R-curve behaviors.[10,12]

Clearly, the large scatter in the measured crack resistance makes it impossible and unreasonable to fit all the data shown in Fig. 2 to a single curve. Thus we fit the experimental data corresponding to each individual crack according to an exponential function proposed by Ramachandran and Shetty[9]

$$K_R = K_\infty - K_0 \exp\left(-\frac{c}{\lambda}\right) \tag{3}$$

where K_∞, K_0 and λ are adjustable parameters.

For each set of data measured with one crack, the best-fit values of the adjustable parameters included in Eq. (3) were obtained by iterative regression minimizing total variance. The results, together with the initial crack length, c_0, measured before crack growth measurements but after the specimens were annealed, are summarized in Table 1. It is shown that, although Eq. (3) gives good fits to the experimentally measured data for each crack, the best-fit values of the three parameters, K_∞, K_0 and λ, in Eq. (3) vary from crack to crack. Note that, even if the initial crack lengths are equal to each other, e.g. cracks C1 and C3 in Table 1, there also exist significant differences in the best-fit values of these three parameters. These findings indicate that the measured R-curve behavior shown in Fig. 2 may be strongly crack-location-dependent.

In general, R-curve behavior for a given material can be characterized simply with three parameters, the threshold crack resistance, K_{th}, the critical crack resistance, K_C, and the crack tolerance, Δc^*, i.e. the difference between the crack lengths corresponding to the critical and the initial states, respectively. Now we wish to examine how the crack location affects the measured R-curve behavior by comparing these three parameters,

Table 1
Best-fit values of the crack-growth-resistance parameters included in Eq. (3)

Indentation load (N)	Crack denotation	c_0 (μm)	K_∞ (MPa$\sqrt{m}$)	K_0 (MPa$\sqrt{m}$)	λ (μm)
196	A1	273.8	12.4	112.0	118.1
	A2	269.4	11.1	179.4	92.4
	A3	275.2	10.1	308.5	77.4
245	B1	311.4	9.5	1991.6	56.6
	B2	323.5	9.6	4037.8	52.4
	B3	328.0	9.2	6062.0	49.6
296	C1	333.2	8.8	2917.3	56.3
	C2	347.6	10.6	235.6	108.0
	C3	334.0	10.8	204.2	109.6

which can be determined empirically from Eq. 3 using the best-fit values listed in Table 1, for different cracks located in different sites in the surface of the test material.

Rewriting Eq. (3) as

$$K_R = K_\infty - K_0 \exp\left(-\frac{c_0}{\lambda}\right)\exp\left(-\frac{\Delta c}{\lambda}\right) \quad (4)$$

where $\Delta c = c_i - c_0$ and c_i is the crack length measured after each loading–unloading cycle. It can be seen that the threshold crack resistance, K_{th}, i.e. the minimum of the applied stress intensity for initiating the stable crack growth, can be obtained by letting $\Delta c = 0$ in Eq. (4). Using the best-fit values listed in Table 1, the K_{th}-values for each crack were calculated and the results are shown in Fig. 3 as a function of the initial crack length, c_0.

Fig. 3 shows that the threshold crack resistance, K_{th}, is nearly independent of the initial crack length or the crack location. Thus it can be concluded that, at least for the material considered in the present study, the threshold resistance may be treated approximately as a crack-location-independent parameter.

Statistical analysis of the nine data shown in Fig. 3 gives an average of 1.2 MPa$\sqrt{m}$ with a standard deviation of 0.2 MPa$\sqrt{m}$. There is reason to believe that this lower K_{th} may be reliable. By directly observing the stable growth of the natural flaws in the surfaces of test specimens, Steinbrech and Schmenkel[1] obtained a K_{th} of about 1.37 MPa$\sqrt{m}$ for a coarse-grained alumina and Marshall and Swain[2] determined $K_{th} = 1.4$ MPa$\sqrt{m}$ for a magnesia-partially-stabilized zirconia (Mg-PSZ). Our result is comparable to these two data and seems to indicate that the annealed indentation-induced cracks may simulate the natural flaws very well.

The existence of a localized microstructural driving force, K_m, for crack growth, which was proposed by Cook et al.[20] to describe the *R*-curve behavior of polycrystalline Al_2O_3, may be considered as the main reason why the threshold resistance for the stable growth of natural flaw is so small and nearly independent of the crack location. Although Cook et al.[20] did not specify the origin of such a localized microstructural driving force, in a following study by Marshall and Swain,[2] it was suggested that, for the Mg-PSZ they examined, K_m may result from the localized transformation near the crack tip. Similarly, we may reasonably assume that, in silicon nitride, K_m may result from the thermal expansion anisotropy of the elongated grains and/or phase transformation of α-$Si_3N_4 \rightarrow \beta$-$Si_3N_4$ during the sintering process. In the early work on the fracture energy of brittle ceramics, Rice and co-workers[21,22] have shown that the internal stresses due to the thermal expansion anisotropy and/or phase transformation are the main causes of the origin of the intrinsic flaws in ceramics.

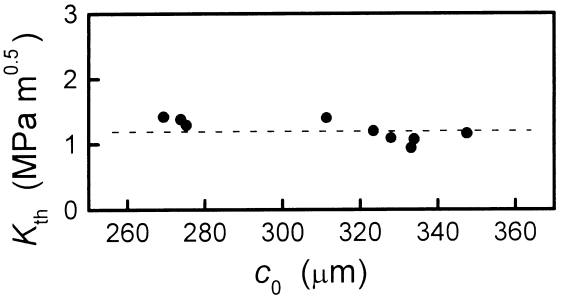

Fig. 3. Threshold crack resistance as a function of the initial crack length.

As proposed by Cook et al.[20] and Marshall and Swain,[2] K_m is a decreasing function of crack extension and can be related to the crack length as

$$K_m = \frac{Q}{c^{3/2}} \quad (5)$$

where Q is a constant that characterizes the intensity of the internal stresses. Note that Eq. (5) has the same form as the stress intensity of residual contact stress due to indentation.[23] One can expect that, after being initiated under the internal stresses, an intrinsic flaw will grow stably until K_m drops to a characteristic value below which no stable crack growth may occur. In other words, any intrinsic flaws may be in a quasi-equilibrium state before being subjected to an applied stress and applying any external stress to the crack will result in a further stable crack growth. If it were the case, the threshold crack resistance for any preexisted flaws in any given ceramic can be expected to be zero. A possible explanation for the fact that the measured K_{th} is somewhat larger than zero can be offered by considering that there is a tendency for a crack which is in a quasi-equilibrium state to be subjected to an environment-assisted slow growth to a certain extent, similar to that observed in the indentation-induced crack system, making K_m reduce slightly.

Now we turn to determine the crack tolerance, Δc^*, from Eq. (3). According to fracture mechanics analysis, the unstable crack growth will occur when the conditions

$$\begin{cases} K_I = K_R \\ \dfrac{dK_I}{dc} \geqslant \dfrac{dK_R}{dc} \end{cases} \quad (6)$$

are satisfied. Substituting Eqs. (1) and (3) into Eq. (6), we obtain

$$\begin{cases} \sigma Y\sqrt{c^*} = K_\infty - K_0 \exp\left(-\dfrac{c^*}{\lambda}\right) \\ \dfrac{1}{2}\sigma Y\sqrt{\dfrac{1}{c^*}} = \left(\dfrac{K_0}{\lambda}\right)\exp\left(-\dfrac{c^*}{\lambda}\right) \end{cases} \quad (7)$$

where c^* is the crack length corresponding to the critical state.

Using the best-fit values of the parameters K_∞, K_0 and λ listed in Table 1, c^* was calculated from Eq. (7) for each crack. The calculated results are given in Table 2. Combining with the initial crack length listed in Table 1, it can be found that the crack tolerance, $\Delta c^* = c^* - c_0$, shows a large scatter, indicating that Δc^* is strongly dependent on the crack location.

Table 2
Calculated crack length and crack resistance corresponding to the critical state

Crack	A1	A2	A3	B1	B2	B3	C1	C2	C3
c^* (μm)	531.9	481.9	462.9	464.3	470.7	470.3	790.9	605.4	593.3
K_C (MPa$\sqrt{m}$)	11.2	10.2	9.3	9.0	9.1	8.8	8.3	9.7	9.8

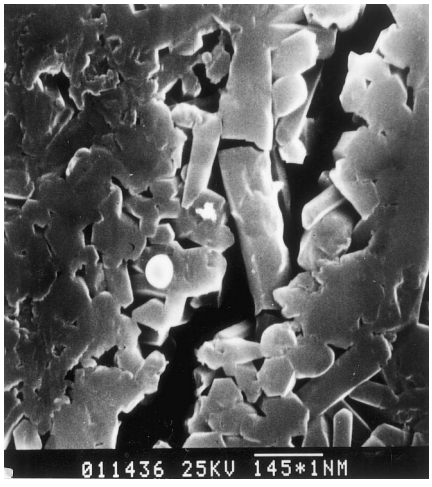

Fig. 4. SEM micrograph showing a bridging grain which has been partially pulled out and fractured.

The crack-location-dependence of crack tolerance can be explained by considering the effect of local microstructural inhomogeneity on crack resistance. As mentioned in Section 1, in monolithic Si_3N_4 ceramics with elongated grain structures, *R*-curve behavior is believed to arise from crack bridging by unbroken grains behind the crack tip. Scanning electron microscopy observations did indicate some evidences of bridging grains in the present Si_3N_4. Fig. 4 shows a bridging grain which has been partially pulled out and fractured. Note that the length direction of this bridging grain is not perpendicular to the crack propagation direction. In fact, as a result of the random orientation of the elongated grains within the material (see Fig. 1), the angle between the length direction of the bridging grain and the crack propagation direction, thereby the interaction between the bridging grains and the propagating crack, may vary from specimen to specimen, from crack to crack, even among different portions of the cracking path of a given crack, resulting in a variation in the crack resistance for different cracks located in different sites in the material surface. Some evidences for this viewpoint may be found in the SEM micrographs shown in Fig. 5.

It is of interest to make a comparison between the crack tolerance, Δc^*, and the experimentally estimated λ values. The variation of Δc^* with λ is shown in Fig. 6. It can be seen that a good linear relationship exists between these two parameters. Following the analysis of Ramachandran and Shetty,[9] the crack-length normalizing parameter, λ, in Eq. (3) may be related empirically to the range of crack extension over which toughening effects should develop and saturate, i.e. the size of the bridging zone behind crack tip. Several authors[3,5,6] have suggested that the crack tolerance, Δc^*, may be related directly to the bridging zone size. Thus, the linear

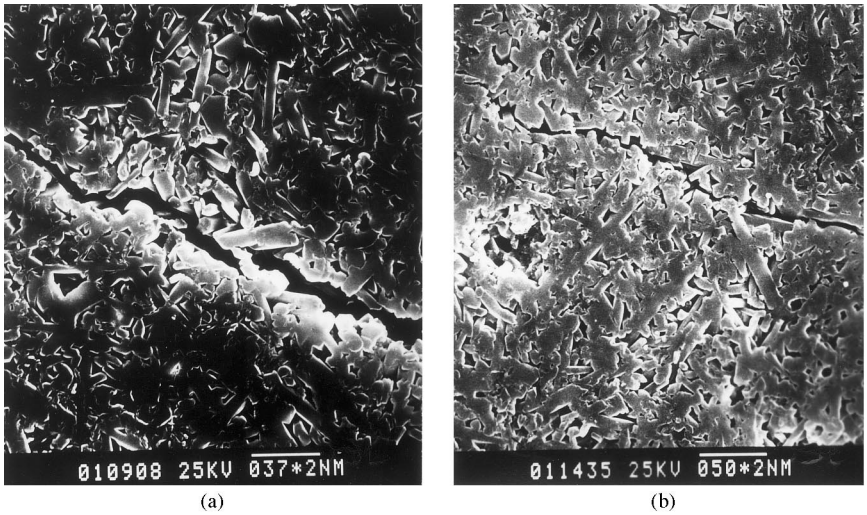

(a) (b)

Fig. 5. SEM micrographs, each showing portion of a remaining indentation-induced crack in the surface of different fractured specimens. Note that the details of the microstructure-crack interactions in these two cracks are somewhat different with each other.

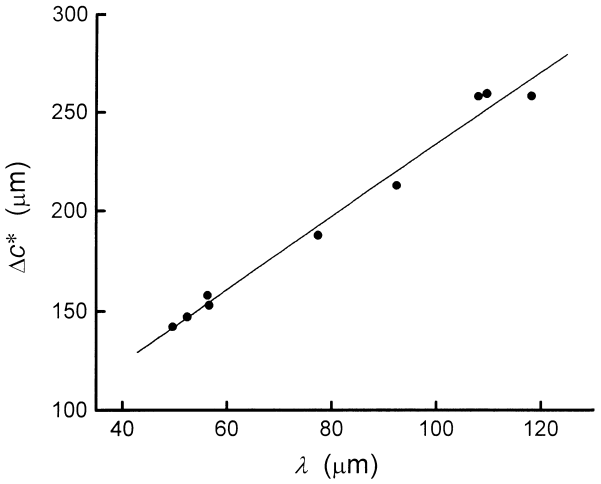

Fig. 6. Variation of the crack tolerance, Δc^*, with the experimentally estimated λ.

relationship shown in Fig. 6 provides a support for the analysis of Ramachandran and Shetty.[9]

The final comment concerns the critical crack resistance, K_C. In continuation of the preceding discussion on Eqs. (6) and (7), the crack resistance corresponding to the critical state, i.e., the critical crack resistance K_C, can be obtained by letting $c = c^*$ in Eq. (1) or Eq. (3). The calculated results of K_C are also given in Table 2. Compared with the threshold crack resistance, K_{th}, a relatively larger scatter exists in the resultant K_C values. Undoubtedly, such a scatter can also be considered as a consequence of the inherent fluctuation in the bridging zone size, as mentioned above.

5. Conclusions

1. The *R*-curve behavior measured with indentation-crack growth method by using an annealed indented specimen shows a strong crack-location dependence. An exponential function proposed by Ramachandran and Shetty can be used to describe the *R*-curve measured with each individual crack.
2. The threshold crack resistance, K_{th}, is found to be crack-location-independent and has a relatively low value. A possible explanation was offered for this phenomenon by considering the existence of a microstructural driving force for crack growth.
3. The crack tolerance, Δc^*, and the critical crack resistance, K_C, are strongly dependent on the crack location. The effect of the random orientation of the elongated grains within the material on the interaction between bridging grain and the propagating crack was suggested to be the main cause of the crack-location-dependence of these two parameters.

References

1. Steinbrech, R. W. and Schmenkel, O., Crack resistance curves of surface cracks in alumina. *J. Am. Ceram. Soc.*, 1988, **71**, C-271–C-273.
2. Marshall, D. B., Swain, M. V., Crack resistance curves in magnesia-partially-stabilized zirconia. *J. Am. Ceram. Soc.*, 1988, **71**, 399–407.
3. Li, C. W., Lee, D. J., Lui, S. C., R-curve behavior and strength for in-situ reinforced silicon nitrides with different microstructures. *J. Am. Ceram. Soc.*, 1992, **75**, 1777–1785.
4. Khan, A., Chan, H. M., Harmer, M. P., Cook, R. F., Toughness-curve behavior of an alumina–mullite composite. *J. Am. Ceram. Soc.*, 1998, **81**, 2613–2623.
5. Evans, A. G., Perspective on the development of high-toughness ceramics, *J. Am. Ceram. Soc.*, 1990, **73**, 187–206.
6. Becher, P. F., Microstructural design of toughened ceramics, *J. Am. Ceram. Soc.*, 1991, **74**, 255–269.
7. Cook, R. F., Clarke, D. R., Fracture stability, R-curves and strength variability. *Acta Metall*, 1988, **36**, 555–562.
8. Shetty, D. K., Wang, J. S., Crack stability and strength distribution of ceramics that exhibit rising crack-growth-resistance (R-curve) behavior. *J. Am. Ceram. Soc.*, 1989, **72**, 1158–1169.
9. Ramachandran, N., Shetty, D. K., Rising crack-growth-resistance (R-curve) behavior of toughened alumina and silicon nitride. *J. Am. Ceram. Soc.*, 1991, **74**, 2634–2641.
10. Cook, S. G., King, J. E., Little, J. A., Surface and subsurface Vickers indentation cracks in SiC, Si_3N_4, and sialon ceramics. *Mater. Sci. Technol.*, 1995, **11**, 1093–1098.
11. Kim, Y. W., Mitomo, M., Hirosaki, N., R-curve behavior of sintered silicon nitride. *J. Mater. Sci.*, 1995, **30**, 4043–4048.
12. Kim, Y. W., Mitomo, M., Hirosaki, N., R-curve behavior and microstructure of sintered silicon nitride. *J. Mater. Sci.*, 1995, **30**, 5178–5184.
13. Cook, R. F. and Lawn, B. R., A modified indentation toughness techniques. *J. Am. Ceram. Soc.*, 1983, **66**, C-200–C-201.
14. Choi, S. R., Salem, J. A., Crack-growth resistance of in situ–toughened silicon nitride. *J. Am. Ceram. Soc.*, 1994, **77**, 1042–1046.
15. Li, C. W., Lui, S. C., Goldacker, J., Relation between strength, microstructure, and grain-bridging characteristics in in situ reinforced silicon nitride. *J. Am. Ceram. Soc.*, 1995, **78**, 449–459.
16. Newman, J. C., Raju, I. S., An empirical stress-intensity factor equation for the surface crack. *Engrg. Fract. Mech*, 1981, **15**, 185–192.
17. Marshall, D. B., Controlled flaws in ceramics: a comparison of Knoop and Vickers indentation. *J. Am. Ceram. Soc.*, 1983, **66**, 127–131.
18. Smith, S. M., Scattergood, R. O., Crack-shape effects for indentation fracture toughness measurements. *J. Am. Ceram. Soc.*, 1992, **75**, 305–315.
19. Steinbrech, R., Knehans, R., Schaarwachter, W., Increase of crack resistance during slow crack growth in Al_2O_3 bend specimens. *J. Mater. Sci.*, 1983, **18**, 265–270.
20. Cook, R. F., Lawn, B. R., Fairbanks, C. J., Microstructure-strength properties in ceramics: I, effect of crack size on toughness. *J. Am. Ceram. Soc.*, 1985, **68**, 604–615.
21. Rice, R. W., Pohanka, R. C., Grain-size dependence of spontaneous cracking in ceramics. *J. Am. Ceram. Soc.*, 1979, **62**, 559–563.
22. Rice, R. W., Pohanka, R. C., McDonough, W. J., Effect of stresses from thermal expansion anisotropy, phase transformations, and second phases on the strength of ceramics. *J. Am. Ceram. Soc.*, 1980, **63**, 703–710.
23. Anstis, G. R., Chantikul, P., Lawn, B. R., Marshall, D. B., A critical evaluation of indentation techniques for measuring fracture toughness: I, direct crack measurements. *J. Am. Ceram. Soc.*, 1981, **64**, 533–538.